Fully Quantum Measurement of the Electron Magnetic Moment

prepared by Maren Padeffke

(presented by N. Herrmann)

Outline

- Motivation and History
- Experimental Methods
- Results
- Conclusion
- Sources

Motivation and History

- Why measure the Electron Magnetic Moment
- Theoretical Prediction of the g Value
- History of g Value Measurements

Why measure the Electron Magnetic Moment

- Electron g – basic property of simplest of elementary particles
-

$$\vec{\mu} = g\mu_B \vec{s}$$

$$\mu_B = \frac{e\hbar}{2m_e c} = 5.788381749(43) \cdot 10^{-11} \frac{MeV}{T}$$

- Determine fine structure constant **α**
  - QED predicts a relationship between g and **α**
- Test QED
  - Comparing the measured electron g to the g calculated from QED using an independent **α**

Theoretical Prediction of the g Value

magnetic moment $\vec{\mu} = g\,\mu_B \frac{\vec{L}}{\hbar}$ ← angular momentum

Bohr magneton $\frac{e\hbar}{2m}$

e.g. What is g for identical charge and mass distributions?

$$\mu = IA = \frac{e}{\left(\frac{2\pi\rho}{v}\right)}(\pi\rho^2) = \frac{ev\rho}{2}\frac{L}{mv\rho} = \frac{e}{2m}L = \frac{e\hbar}{2m}\frac{L}{\hbar}$$

($\frac{e\hbar}{2m} = \mu_B$)

$\rightarrow \quad g = 1$

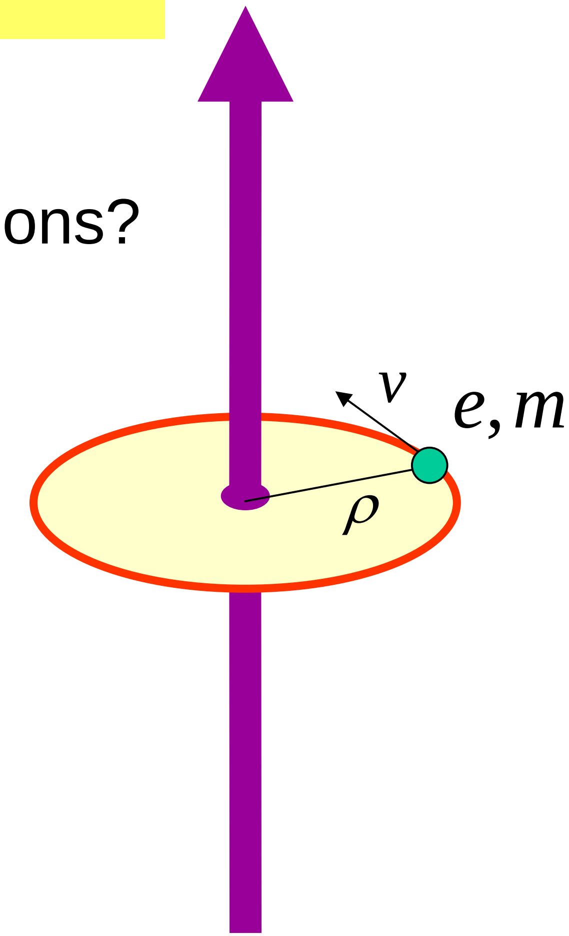

Feynman diagrams

Dirac particle: g=2

Each vertex contributes $\sqrt{\alpha}$

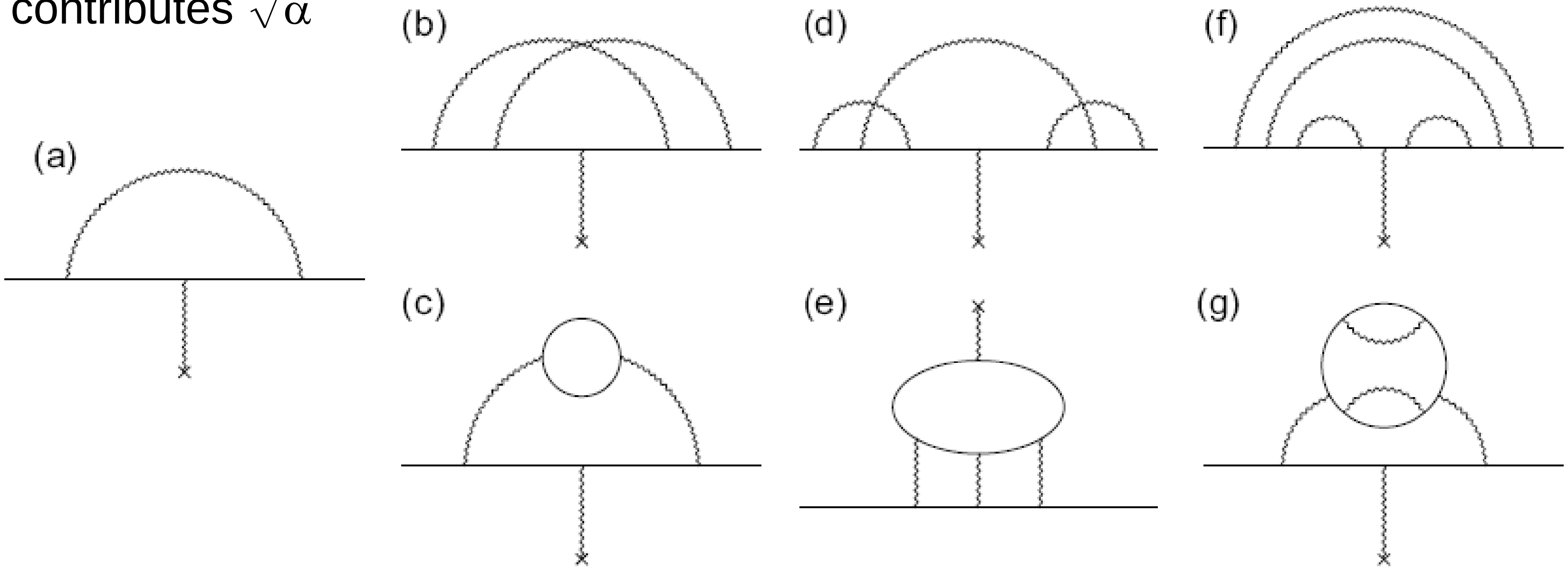

Figure 1.2: The second-order Feynman diagram (a), 2 of the 7 fourth-order diagrams (b,c), 2 of 72 sixth-order diagrams (d,e), and 2 of 891 eighth-order diagrams (f,g).

QED corrections

(added by NH)

Dirac+QED Relates Measured g

$$\frac{g}{2} = 1 + C_1\left(\frac{\alpha}{\pi}\right) + C_2\left(\frac{\alpha}{\pi}\right)^2 + C_3\left(\frac{\alpha}{\pi}\right)^3 + C_4\left(\frac{\alpha}{\pi}\right)^4 + \ldots \delta a$$

Measure

Dirac point particle

QED Calculation

Kinoshita, Nio, Remiddi, Laporta, etc.

weak/strong

Sensitivity to other physics (weak, strong, new) is low

- $C_1 = 0.5$
- $C_2 = -0.328\ldots$ (7 Feynman diagrams) analytical
- $C_3 = 1.181\ldots$ (72 Feynman diagrams) analytical
- $C_4 \sim -1.71$ (involving 891 four-loop Feynman diagrams) numerical

$$\frac{g}{2} = 1 + C_1\left(\frac{\alpha}{\pi}\right) + C_2\left(\frac{\alpha}{\pi}\right)^2 + C_3\left(\frac{\alpha}{\pi}\right)^3 + C_4\left(\frac{\alpha}{\pi}\right)^4 + \ldots\ \delta a$$

theoretical uncertainties

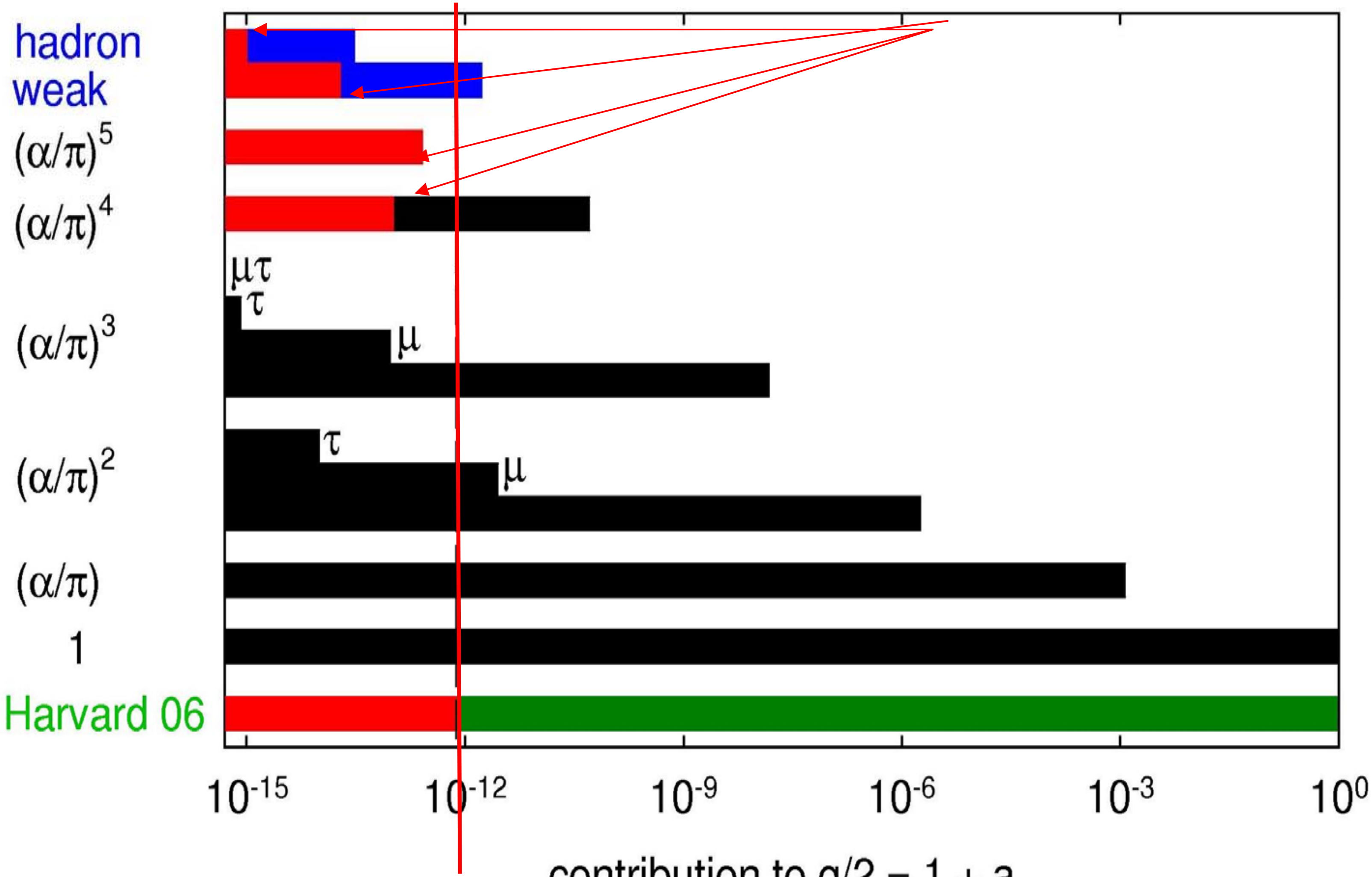

experimental uncertainty

Basking in the Reflected Glow of Theorists

$$\frac{g}{2} = 1 + C_1\left(\frac{\alpha}{\pi}\right) + C_2\left(\frac{\alpha}{\pi}\right)^2 + C_3\left(\frac{\alpha}{\pi}\right)^3 + C_4\left(\frac{\alpha}{\pi}\right)^4 + C_5\left(\frac{\alpha}{\pi}\right)^5 + \ldots \delta a$$

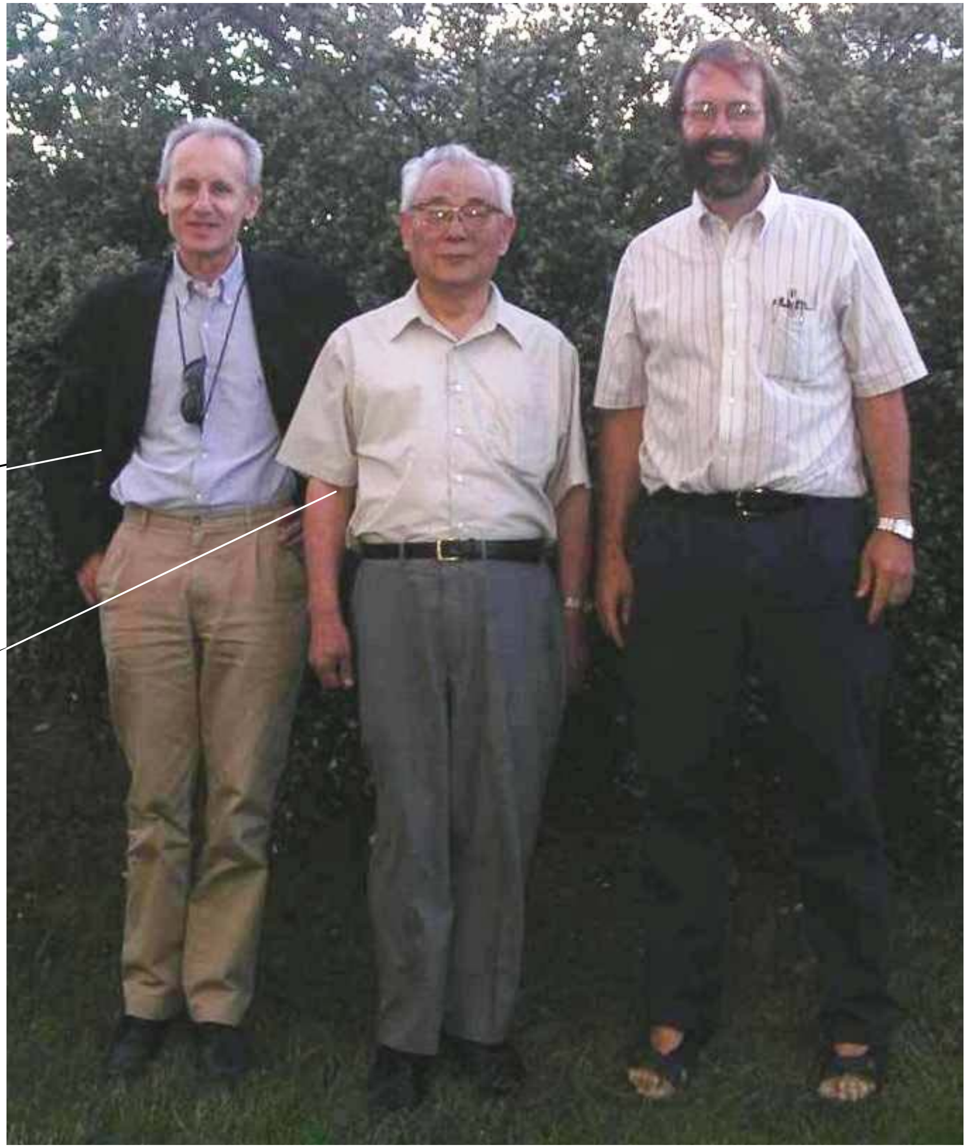

2004

Remiddi Kinoshita G.Gabrielse

History of g Value Measurements

U. Michigan

beam of electrons

spins precess with respect to cyclotron motion

Crane, Rich, …

U. Washington

one electron

observe spin flip

thermal cyclotron motion

Dehmelt, Van Dyck

Harvard

one electron

quantum cyclotron motion

resolve lowest quantum levels

cavity-controlled radiation field (cylindrical trap)

100 mK

self-excited oscillator

inhibit spontan. emission

cavity shifts

History of the Measured Values

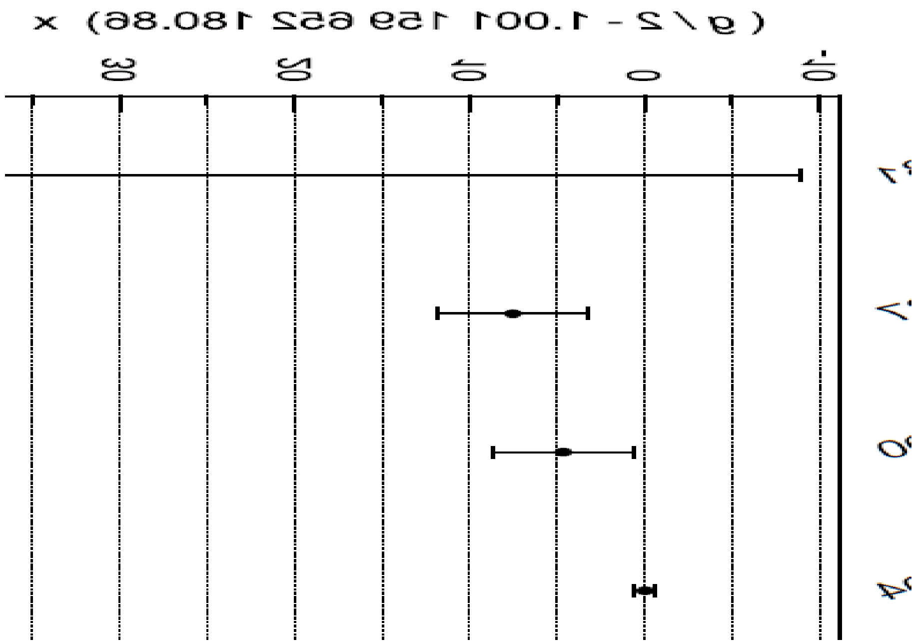

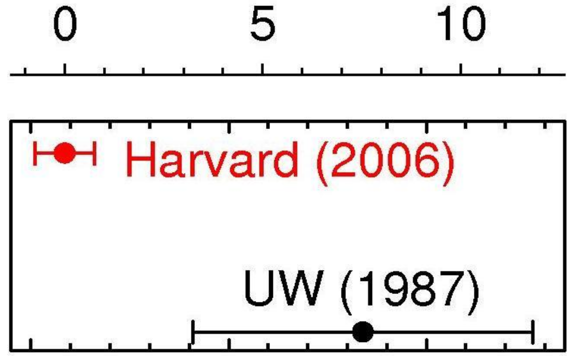

Experimental Methods

- g Value Measurement Basics
- Single Quantum Spectroscopy and Sub-Kelvin
- Cyclotron Temperature
- Sub-Kelvin Axial Temperature
- Cylindrical Penning Trap
- Magnetic Field Stability
- Measurements

g Value Measurement: Basics

Quantum jump spectroscopy of lowest cyclotron and spin levels of an electron in a magnetic field

cool 12 kHz

200 MHz detect

- very small accelerator
- designer atom

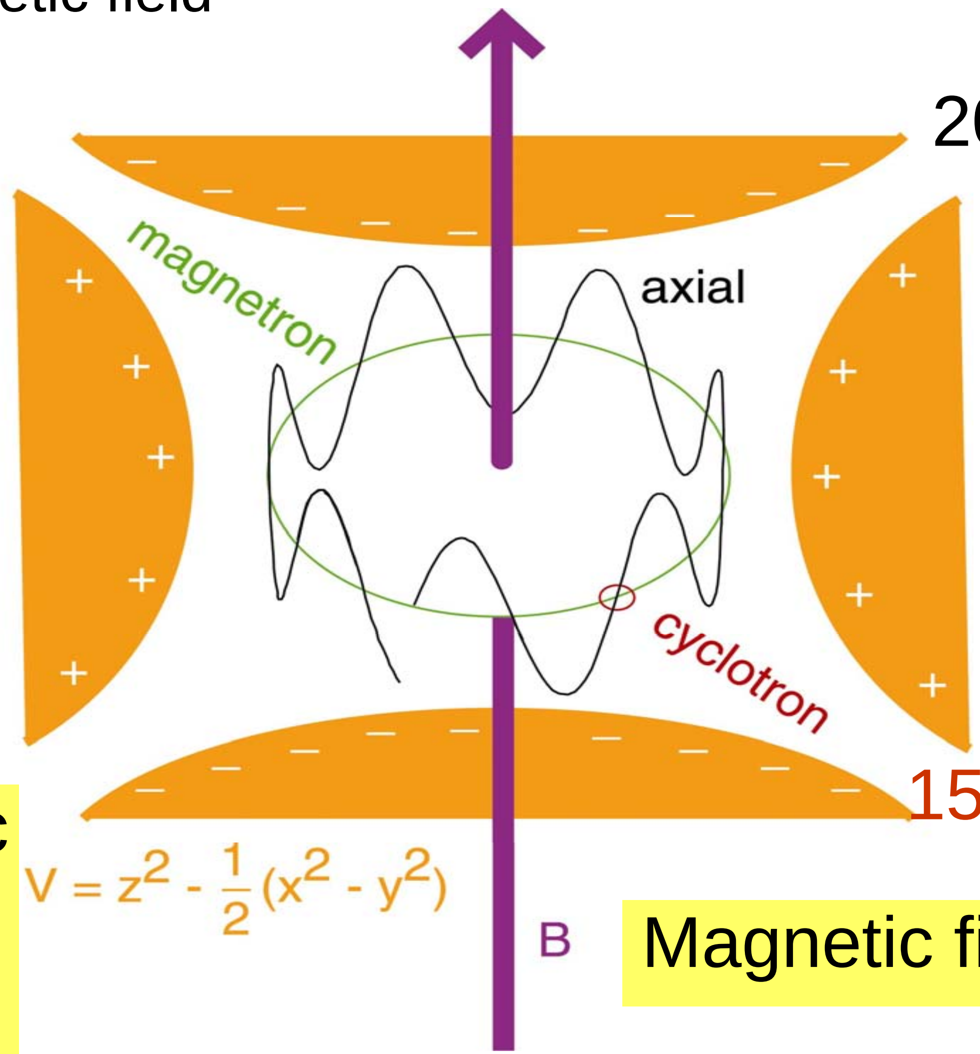

153 GHz

need to measure for g/2

Electrostatic quadrupole potential

Magnetic field

- Quantized motions of a single electron in a
- Penning Trap (without special relativity)

- since $g \neq 2$, $\boldsymbol{\omega_c}$ and $\boldsymbol{\omega_s}$ are not equal $\longrightarrow$ non-zero anomaly shift $\boldsymbol{\omega_a}$
- g could be determined by measurement of cyclotron and spin frequency: $\mathbf{g/2 = \omega_s/\omega_c \approx 1}$

$$\nu_c = \frac{1}{2\pi}\frac{eB}{m} \qquad \nu_s = \frac{g}{2}\nu_c$$

- g-2 can be obtained directly from cyclotron and anomaly frequencies: ~~$\mathbf{g/2 - 1 = \omega_s/\omega_c \approx 1X10^{-3}}$~~

$$\mathbf{g/2 - 1 = (\omega_s - \omega_c)/\omega_c = \omega_a/\omega_c \approx 1X10^{-3}}$$

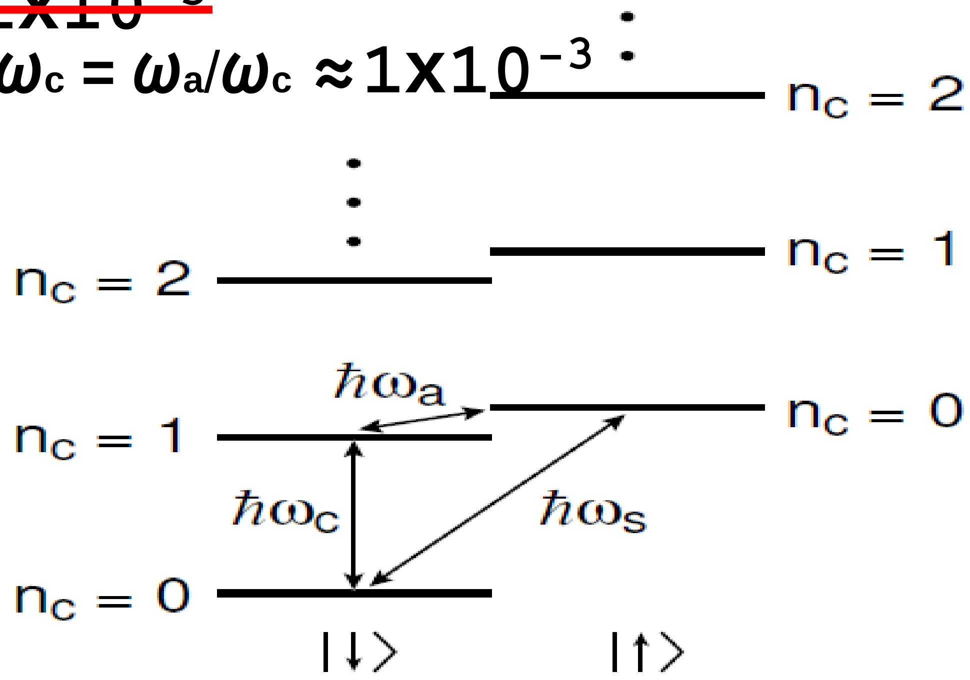

$\longrightarrow$ g-2 experiments gain three orders of magnitude in precision over g experiments

Experimental key feature

PRL **97,** 030801 (2006) PHYSICAL REVIEW LETTERS week ending 21 JULY 2006

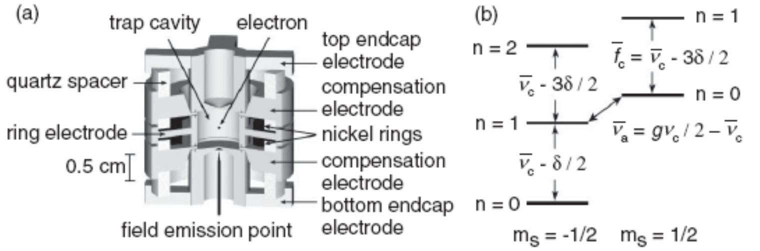

FIG. 2. Cylindrical Penning trap cavity used to confine a single electron and inhibit spontaneous emission (a), and the cyclotron and spin levels of an electron confined within it (b).

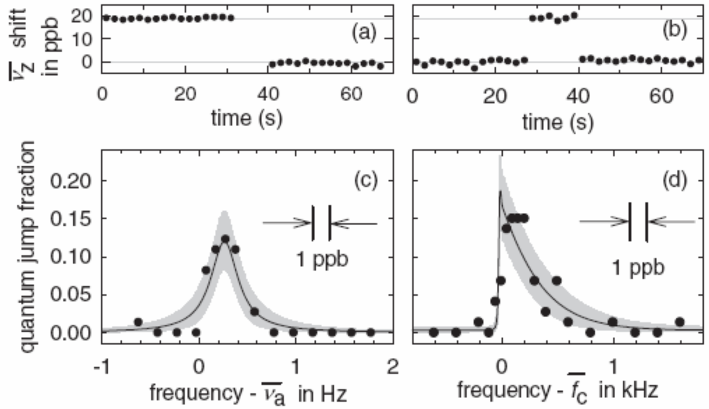

FIG. 3. Sample $\bar{\nu}_z$ shifts for a spin flip (a) and for a one-quantum cyclotron excitation (b). Quantum jump spectroscopy line shapes for anomaly (c) and cyclotron (d) transitions, with a maximum likelihood fit to the calculated line shapes (solid). The bands indicate 68% confidence limits for distributions of measurements about the fit values.

would damp in ~0.1 s via synchrotron radiation in free space. This spontaneous emission is greatly inhibited in the trap cavity (to 6.7 or 1.4 s here) when **B** is tuned so $\bar{\nu}_c$ is far from resonance with cavity radiation modes [7,15]. Blackbody photons that would excite the cyclotron ground state are eliminated by cooling the trap and vacuum enclosure below 100 mK with a dilution refrigerator [6]. (Thermal radiation through the microwave inlet makes <1 excitation/h.) The axial motion, damped by a resonant circuit, cools below 0.3 K (from 5 K) when the axial detection amplifier is off for crucial periods. The magnetron motion radius is minimized with axial sideband cooling [15].

For the first time, g is deduced from observed transitions between only the lowest of the spin ($m_s = \pm 1/2$) and cyclotron ($n = 0, 1, 2, \ldots$) energy levels [Fig. 2(b)],

$$E(n, m_s) = \frac{g}{2} h\nu_c m_s + \left(n + \frac{1}{2}\right)h\bar{\nu}_c - \frac{1}{2}h\delta\left(n + \frac{1}{2} + m_s\right)^2.$$

circuit that is amplified and fed back to drive the oscillation. QND couplings of spin and cyclotron energies to $\bar{\nu}_z$ [6] arise because saturated nickel rings [Fig. 2(a)] produce a small magnetic bottle, $\Delta\mathbf{B} = \beta_2[(z^2 - \rho^2/2)\hat{\mathbf{z}} - z\rho\hat{\boldsymbol{\rho}}]$ with $\beta_2 = 1540\ \mathrm{T/m^2}$.

Anomaly transitions are induced by applying potentials oscillating at $\bar{\nu}_a$ to electrodes, to drive an off-resonance axial motion through the bottle's $z\boldsymbol{\rho}$ gradient. The electron sees the oscillating magnetic field perpendicular to **B** as needed to flip its spin, with a gradient that allows a simultaneous cyclotron transition. Cyclotron transitions are induced by microwaves with a transverse electric field that

(added by NH)

Single Quantum Spectroscopy and Sub-Kelvin Cyclotron Temperature

- cooling trap cavity to sub-Kelvin temperatures ensures that cyclotron oscillator is always in ground state (no blackbody radiation)
- relativistic frequency shift between two lowest quantum states is precisely known

Average number of blackbody photons in the cavity

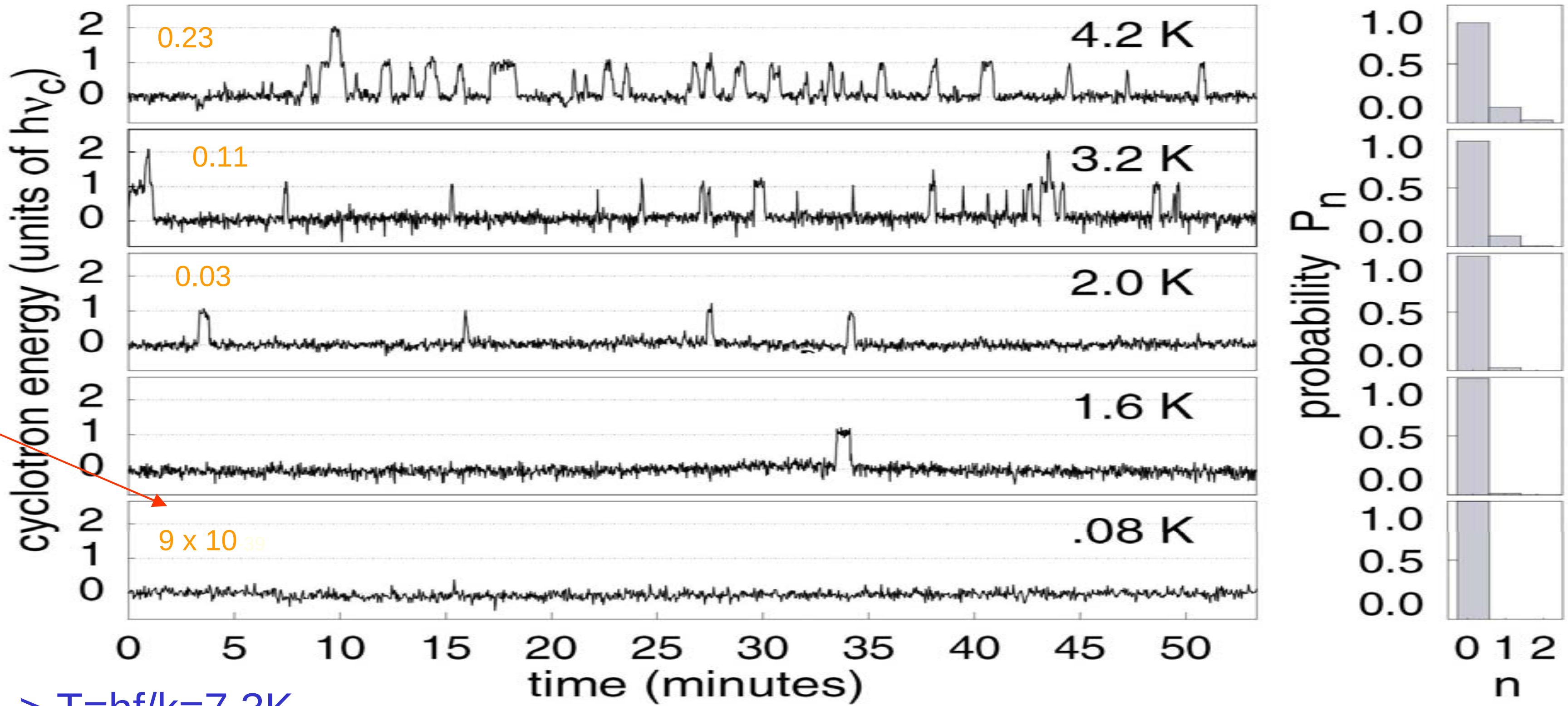

Note: 153 GHz -> T=hf/k=7.3K

Sub-Kelvin Axial Temperature

- Anomaly and cyclotron resonance acquire an inhomogeneous
- broadening proportional to the temperature T_z of the electron's
- axial motion
  - Occurs because a magnetic inhomogeneity is introduced to allow detection of spin and cyclotron transition

- cooling T_z to sub-Kelvin narrows the cyclotron and anomaly line
- widths

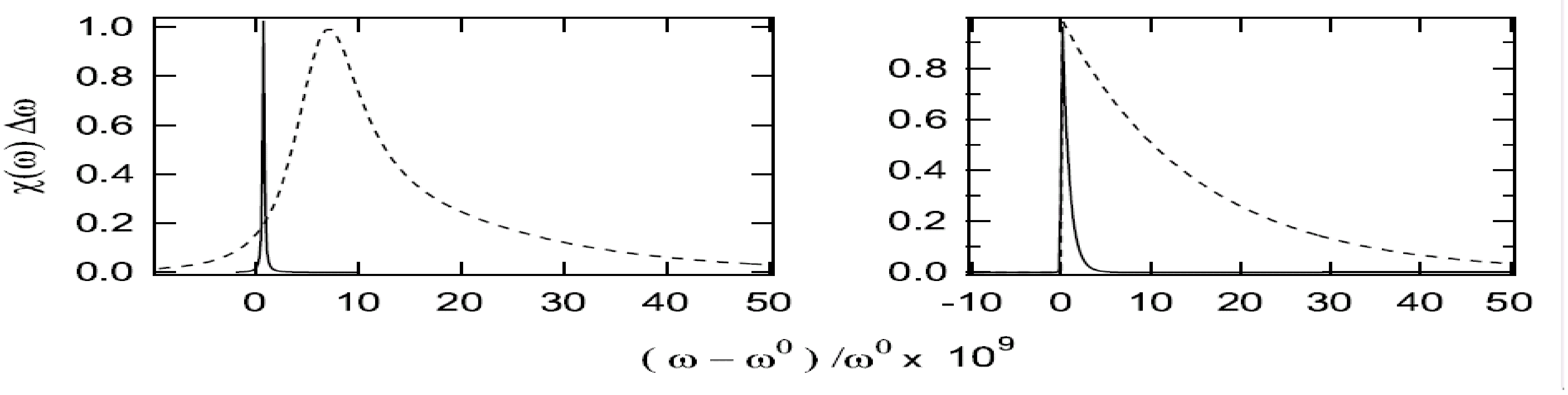

anomaly (left) and cyclotron (right) with T_z = 5 K (dashed) and T_z = 300 mK (solid)

Cylindrical Penning Trap

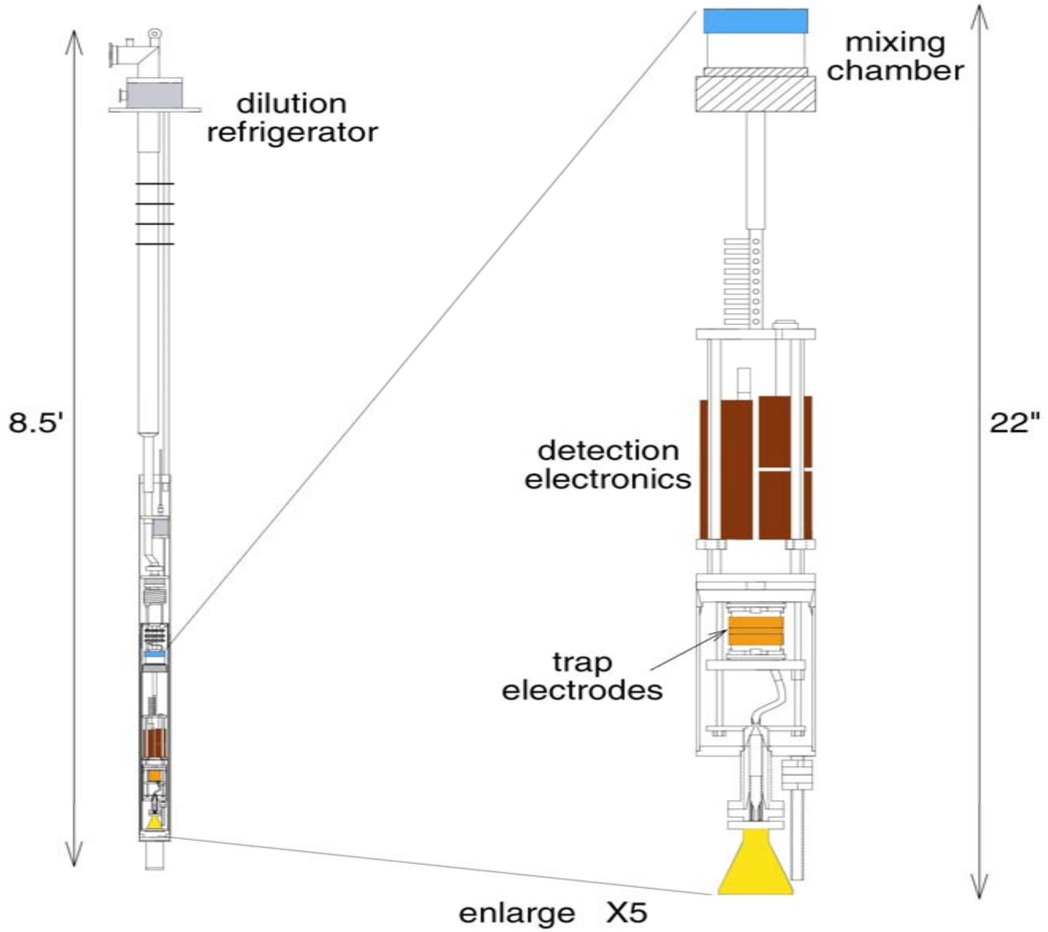

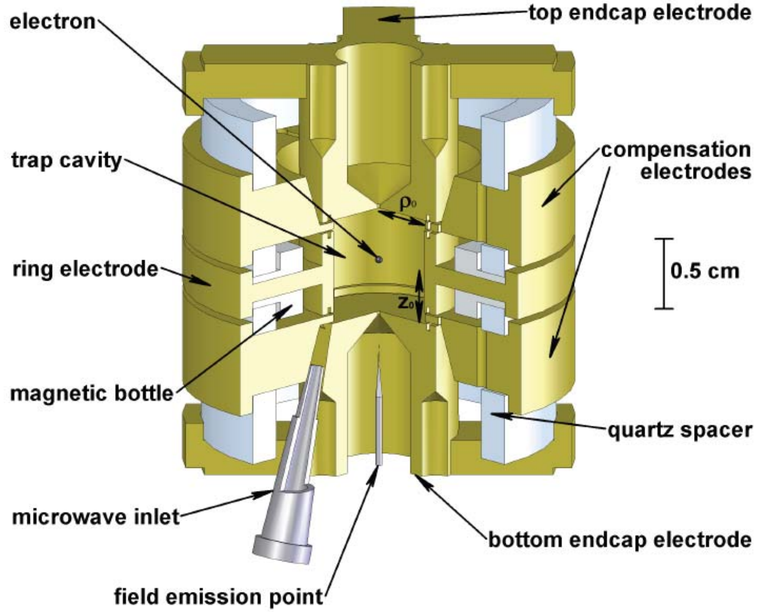

David Hanneke G.Gabrielse

Measurement procedure

Anomaly transitions are induced by applying potentials oscillating at $\bar{\nu}_a$ to electrodes, to drive an off-resonance axial motion through the bottle's $z\boldsymbol{\rho}$ gradient. The electron sees the oscillating magnetic field perpendicular to $\mathbf{B}$ as needed to flip its spin, with a gradient that allows a simultaneous cyclotron transition. Cyclotron transitions are induced by microwaves with a transverse electric field that are injected into and filtered by the cavity. The electron samples the same magnetic gradient while $\bar{\nu}_a$ and $\bar{f}_c$ transitions are driven, because both drives are kept on, with one detuned slightly so that only the other causes transitions.

A measurement starts with the SEO turned on to verify that the electron is in the upper of the two stable ground states, $|n = 0, m_s = 1/2\rangle$. Simultaneous $\bar{\nu}_c - \delta/2$ and $\bar{\nu}_a$ drives prepare this state as needed. The magnetron radius is reduced with 1.5 s of strong sideband cooling [15] at $\bar{\nu}_z + \bar{\nu}_m$, and the detection amplifier is turned off. After 1 s, either an $\bar{f}_c$ drive, or a $\bar{\nu}_a$ drive, is on for 2 s. The detection amplifier and the SEO are then switched on to check for a cyclotron excitation, or a spin flip (from an anomaly transition followed by a cyclotron decay). Inhibited spontaneous emission gives the time needed to observe a cyclotron excitation before an excited state decays. We step through each $\bar{\nu}_c$ and $\bar{\nu}_a$ drive frequency in turn, recording the number of quantum jumps per drive attempt. This measurement cycle is repeated during nighttimes, when electrical and magnetic noise are lower. A low drive strength keeps the transition probability below 20% to avoid saturation effects.

PRL 97, 030801 (2006)

Quantum jump spectroscopy

Probablility to change state as function of detuning of drive frequency

(NH)

Quantum nondemolition measurement

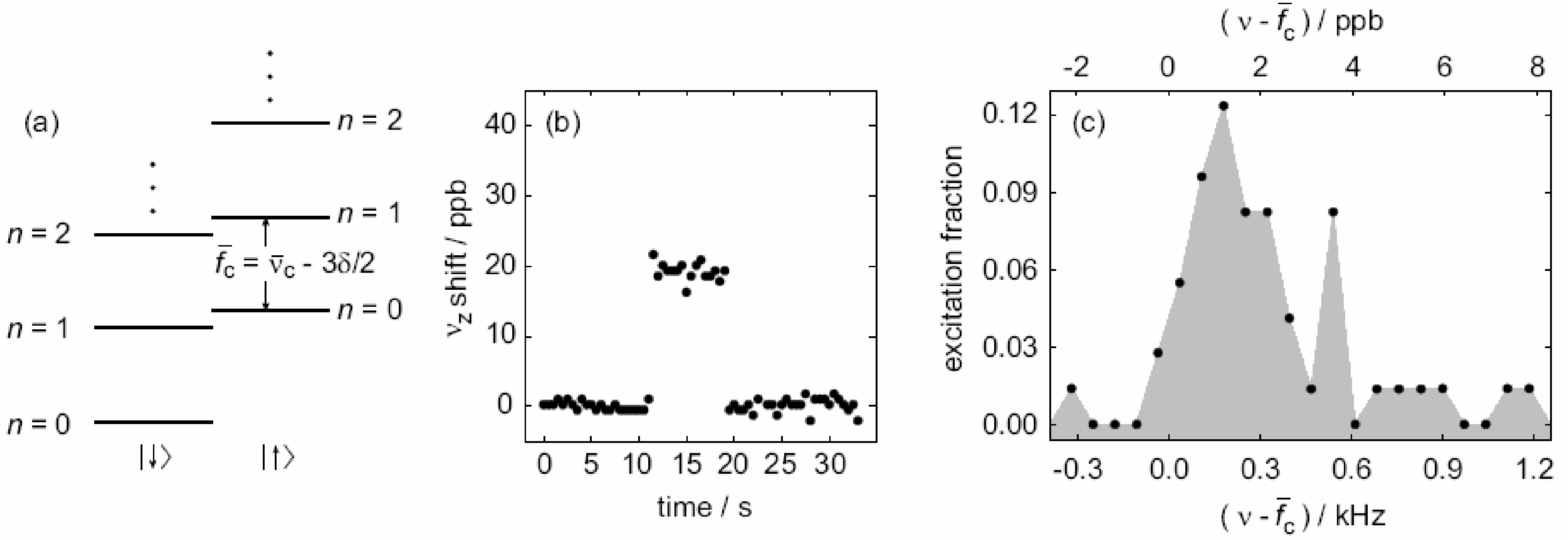

Figure 4.4: Cyclotron quantum jump spectroscopy proceeds through discrete interrogations of the lowest cyclotron transition in the spin-up ladder (a). A successful excitation appears as a shift in the axial frequency (b), a quantum nondemolition measurement technique. Multiple attempts at different frequencies may be binned into a histogram (c) to reveal the overall cyclotron line.

(NH)

Advantages of a Cylindrical Penning Trap

- well-understood electromagnetic cavity mode structures
- reducing the difficulties of machining the electrodes
- cavity modes of cylindrical traps are expected to have higher Q values and a lower spectral density than those of hyperbolic traps
  - $\longrightarrow$ allows better detuning of cyclotron oscillator, which causes an inhibition of cyclotron spontaneous emission
- frequency-shift systematics can be better controlled
  - $\longrightarrow$ these shifts in the cyclotron frequency were the leading sources of uncertainty in the 1987 University of Washington g value measurements

Magnetic Field Stability

- in practice, measuring the cyclotron and anomaly frequencies
- takes several hours
- ⟶ temporal stability of magnetic field is very important

- trap center must not move significantly relative to the
- homogeneous region of the trapping field

- magnetism of the trap material themselves must be stable

- pressure and temperature must be well-regulated

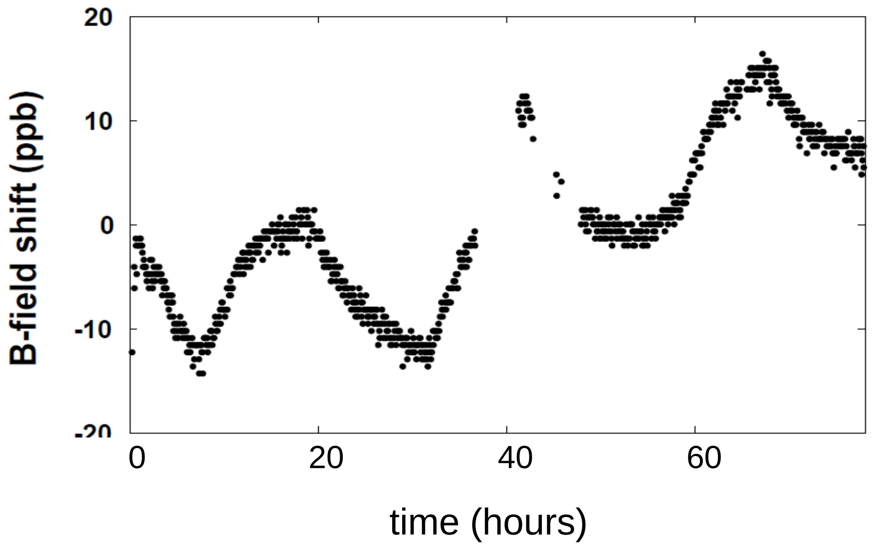

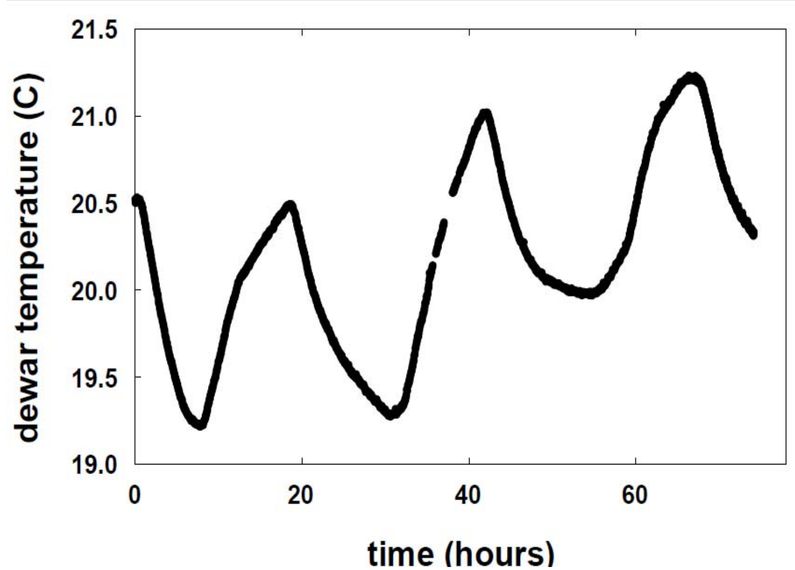

Eliminate Nuclear Paramagnetism

- attempts to regulate the temperature and heat flows could not
- make sufficient precise for line widths an order of magnitude
- narrower
- $\longrightarrow$ entire trap apparatus was rebuilt from materials with smaller nuclear paramagnetism

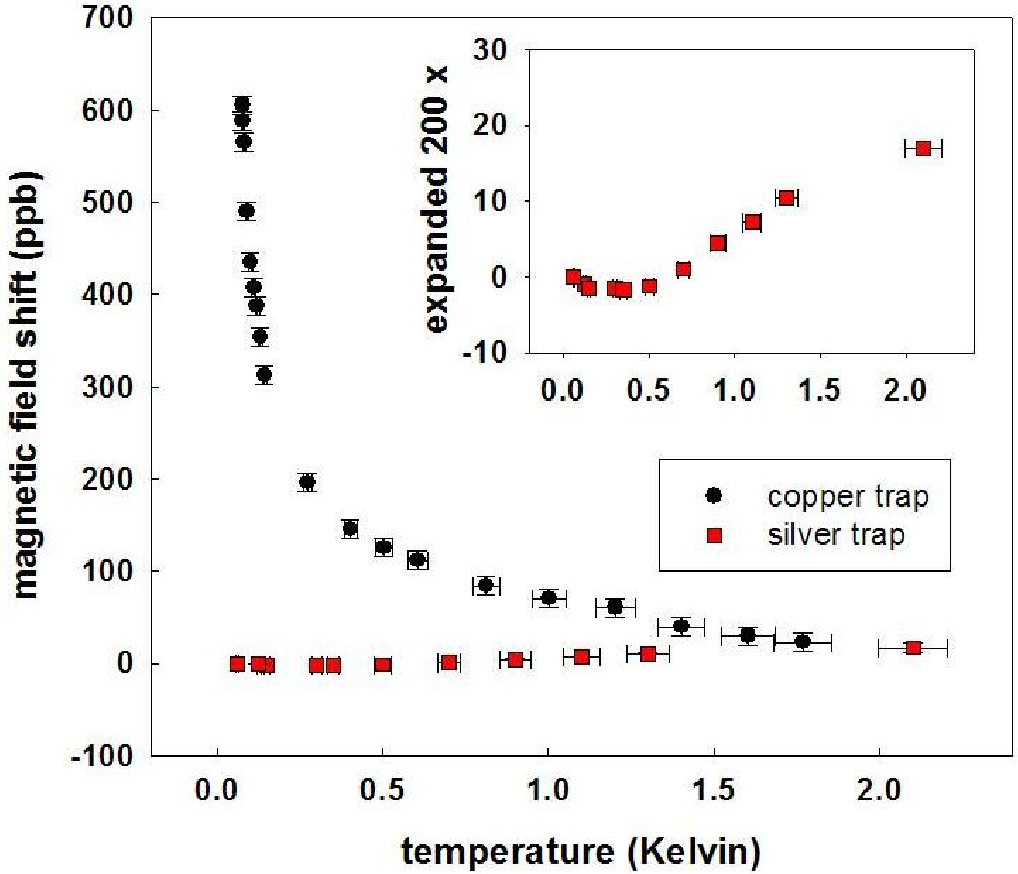

Measurements

- due to a coupling to the axial motion, the magnetron, cyclotron,
- and spin energy changes can be detected as shifts in the axial
- frequency

- the measurements from Harvard University were taken at

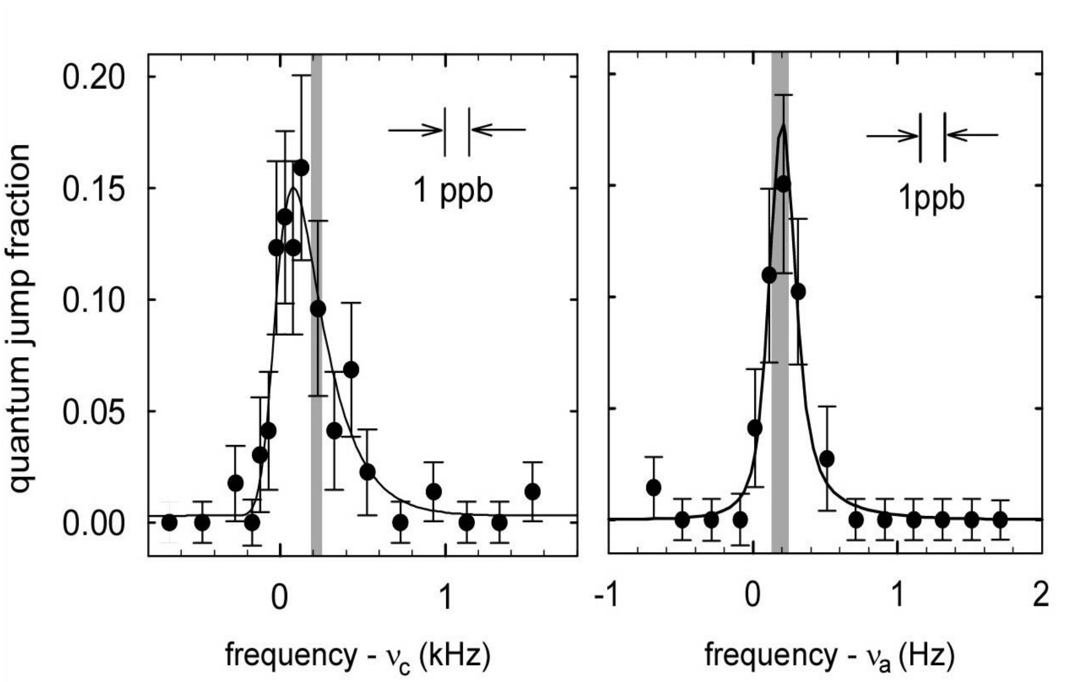

cyclotron **anomaly**

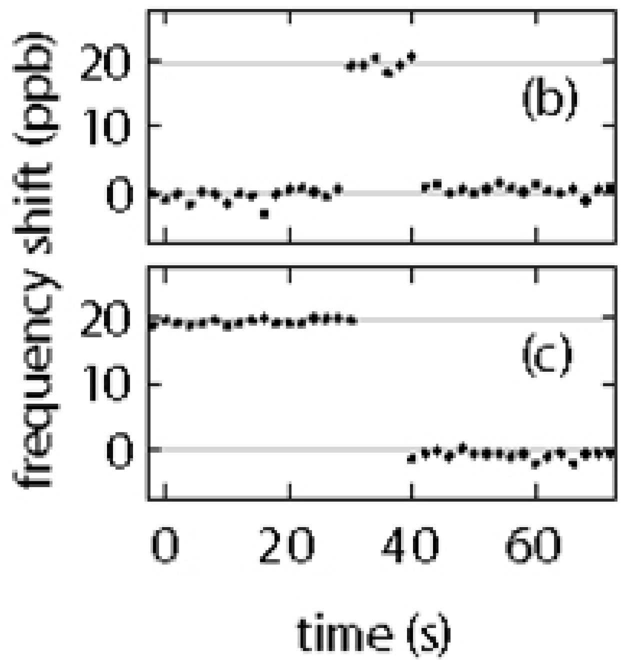

one quantum cyclotron excitation

spin flip

Results

Uncertainties

- Non-parenthesized: corrections applied to obtain correct value for g,
- parenthesized: uncertainties

source	$\Delta g/g \times 10^{12}$ at 146.8 GHz	$\Delta g/g \times 10^{12}$ at 149.0 GHz
relativistic $\Delta\nu_c$	– 2.07 (0.00)	– 2.10 (0.00)
misalignment	0.00 (0.00)	0.00 (0.00)
ν_z anharmonicity	0.2 (0.3)	0.00 (0.02)
anomaly power	0.0 (0.4)	0.00 (0.14)
cyclotron power	0.0 (0.3)	0.00 (0.12)
cavity shift	10.2 (6.0)	–0.07 (0.52)
total corrections	**8.3 (6.0)**	**-2.17 (0.55)**

g -values

- First parenthesis statistic, second systematic uncertainty

ν_c	$g/2$ without cavity corrections	$g/2$ with cavity corrections
146.8 GHz	1.001 159 652 171 48 (12) (58)	1.001 159 652 181 68 (12) (600)
149.0 GHz	1.001 159 652 180 93 (15) (19)	1.001 159 652 180 86 (15) (55)
wtd. mean		1.001 159 652 180 87 (57)

From 2004 to 2008

$g/2 = 1.001\ 159\ 652\ 180\ 86(57)$

$g/2 = 1.001\ 159\ 652\ 180\ 85(76)$

$g/2 = 1.001\ 159\ 652\ 180\ 73(28)$

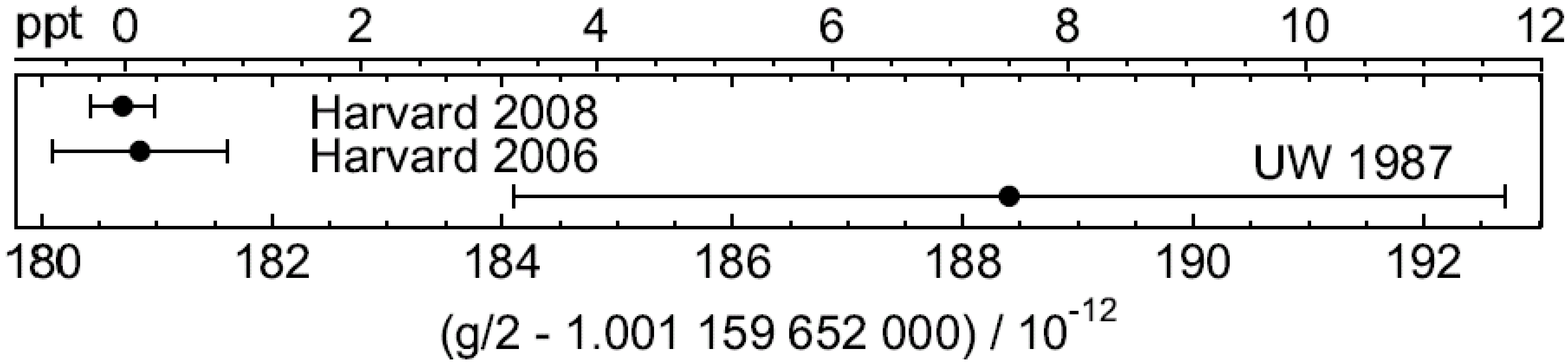

Conclusion

How Does One Measure g to some Parts in 10^{-12} ?

→ Use New Methods

first measurement with these new methods

- One-electron quantum cyclotron
- Resolve lowest cyclotron as well as spin states
- Quantum jump spectroscopy of lowest quantum states
- Cavity-controlled spontaneous emission
- Radiation field controlled by cylindrical trap cavity
- Cooling away of blackbody photons
- Synchronized electrons probe cavity radiation modes
- Trap without nuclear paramagnetism
- One-particle self-excited oscillator

Sources

hussel.harvard.edu/~gabrielse/gabrielse/papers/2004/OdomThesis.pdf

http://hussle.harvard.edu/~hanneke/CV/2007/Hanneke-HarvardPhD_Thesis.pdf

www.phys.uconn.edu/icap2008/invited/icap2008-gabrielse.pdf

vmsstreamer1.fnal.gov/VMS_Site_03/Lectures/Colloquium/presetatins/070124 Gabrielse.ppt